Warp propagation in thin accretion discs

Daniel Price (Monash)
Giuseppe Lodato (Milan)

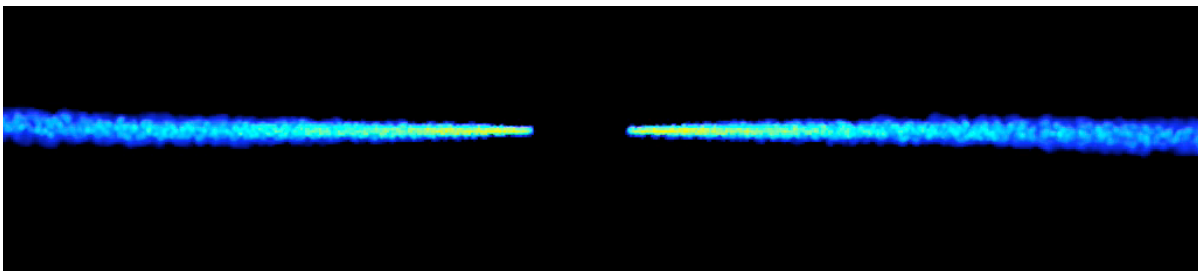

Warped accretion discs

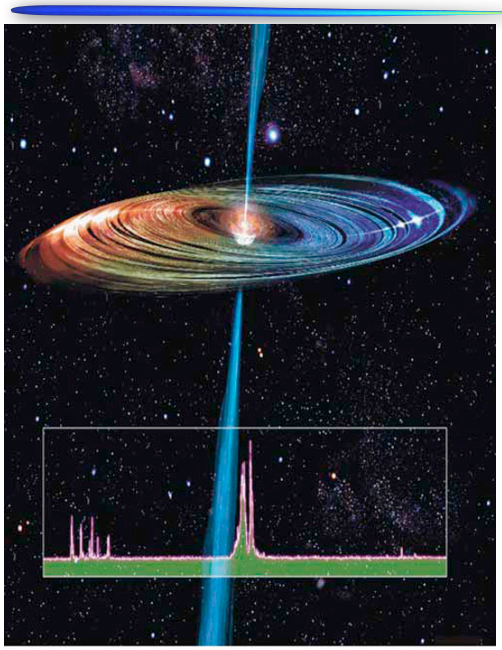

An artist's impression of an accretion disk surrounding a super-massive black hole. Masers appear in the disk in front of the black hole as well as along a line where the disk is moving directly toward or away from us. This results in a characteristic triple-peaked signature as seen in the lower part of the figure.

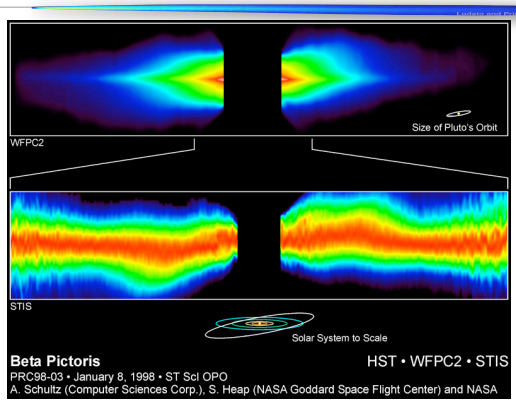

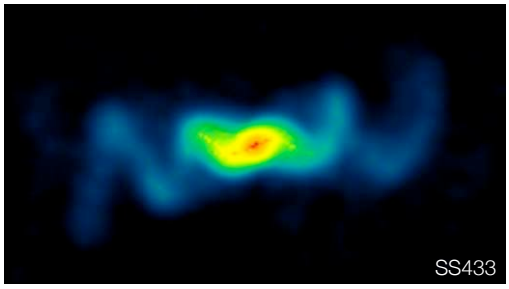

Observed warps in accretion discs

- X-ray binaries: SS433 (Begelman et al. 2006)
- Microquasars: GROJ1655-40 (Martin et al. 2008a), V4641 Sgr (Martin et al. 2008b)
- Protostellar discs: KH 15D (Chiang & Murray-Clay 2004)
- AGN: NGC4258 (Herrnstein et al. 1996, Papaloizou et al. 1998), Centaurus A

Standard disc theory

Shakura-Sunyaev (1973), Pringle (1981)

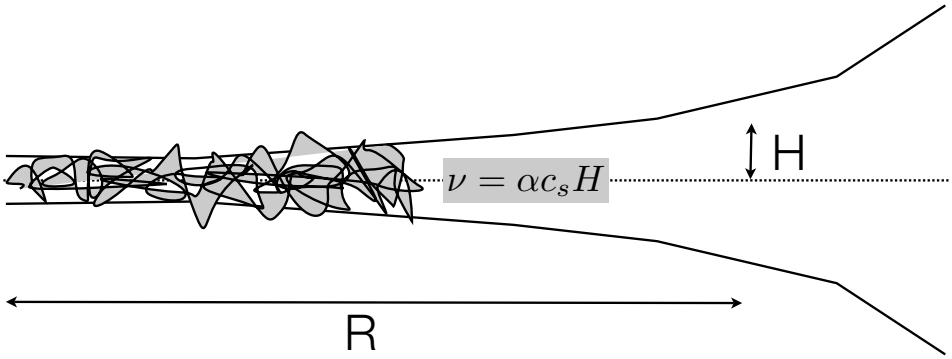

Warped disc theory

- define angular momentum vector L for each disc annulus
- for a Keplerian disc: $L(R) = \Sigma(R)\sqrt{GMR}$
- unit vector:

$$\mathbf{l}(R) = \frac{\mathbf{L}(R)}{L(R)}$$

- disc is warped if direction of l changes with radius

Theory of warp propagation

- Papaloizou & Pringle (1983):

$\frac{H}{R} \gtrsim \alpha$: warp propagates like a bending wave

(applies to thick and/or low viscosity discs)

$\frac{H}{R} \lesssim \alpha$: warp propagates diffusively

(applies to thin and/or high viscosity discs)

(protostellar, AGN, microquasars...)

Diffusive warp propagation

- Define “warp viscosity” similar to disc viscosity

$$\nu_2 = \alpha_2 c_s H$$

- work out α_2 as a function of α

Warp diffusion: theory

- Papaloizou & Pringle (1983) found that for small amplitude warps in thin (H/R << alpha) discs at low alpha:

$$\alpha_2 = \frac{1}{2\alpha} + \mathcal{O}(\alpha^2, \psi)$$

- this has not (yet) been confirmed by numerical simulations

- Ogilvie (1999) gives higher order corrections for finite α (but small warps)

$$\frac{\nu_2}{\nu_1} = \frac{1}{2\alpha^2}\frac{4(1+7\alpha^2)}{4+\alpha^2} + \mathcal{O}(\psi)$$

3D simulations

- Solve equations of viscous gas dynamics in 3D assuming a Shakura-Sunyaev type viscosity:

$$\frac{d\rho}{dt} = -\rho\nabla\cdot\mathbf{v},$$

$$\frac{dv^i}{dt} = -\frac{1}{\rho}\frac{\partial S^{ij}}{\partial x^j} + f^i_{\rm pot}, \qquad \mathbf{f}_{\rm pot} = -\frac{GM}{r^2}\hat{\mathbf{r}},$$

$$S^{ij} = \left[-P + \left(\zeta - \frac{2}{3}\eta\right)\frac{\partial v^k}{\partial x^k}\right]\delta^{ij} + \eta\left(\frac{\partial v^i}{\partial x^j} + \frac{\partial v^j}{\partial x^i}\right),$$

$$\nu = \eta/\rho = \alpha c_s(R)H \qquad \zeta = 0$$

$$P = c_{\rm s}^2(R)\rho, \qquad c_{\rm s}(R) = c_{\rm s,0}R^{-3/4},$$

Smoothed Particle Hydrodynamics

Lucy (1977), Gingold & Monaghan (1977), Monaghan (1992), Price (2004), Monaghan (2005)

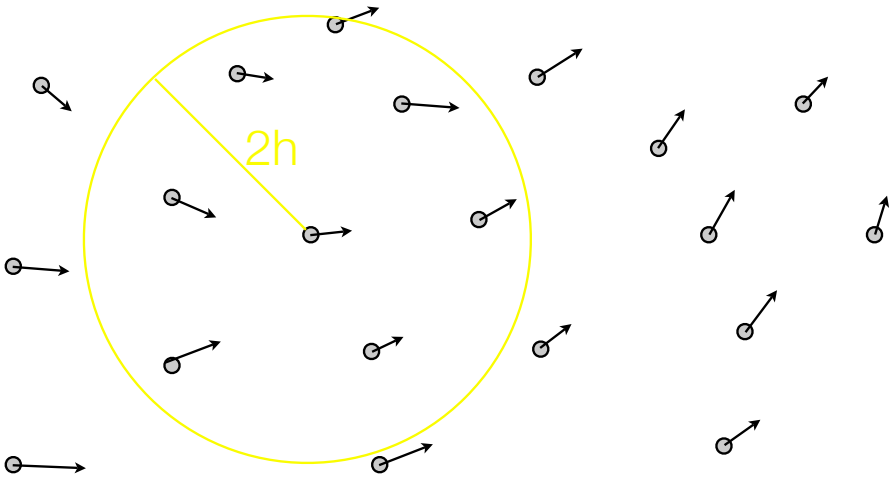

$$\rho(r_i) = \sum_j m_j W(r_i - r_j, h)$$

Viscosity in SPH

- Artificial viscosity term is known to represent Navier-Stokes viscosity (Monaghan 1985, Lubow 1994, Murray 1996):

$$\nu^{\rm AV} \approx \frac{1}{10}\alpha^{\rm AV} c_{\rm s} h, \qquad \alpha \approx \frac{1}{10}\alpha^{\rm AV}\frac{\langle h\rangle}{H},$$
$$\zeta_v^{\rm AV} \approx \frac{1}{6}\alpha^{\rm AV} c_{\rm s} h.$$

  - apply for both approaching and receding particles
  - use $v_{sig} = c_s$
  - do not use switches to turn viscosity on/off
  - turn off non-linear beta term
  - setup disc such that h/H ~ const

- An alternative is to implement the Navier-Stokes terms directly by computing two first derivatives (e.g. Flebbe et al. 1994). Advantage is control over ratio of shear-to-bulk viscosity.

PHANTOM

- low memory, highly efficient SPH code for non-self-gravitating problems
- uses fixed grid neighbour-finding instead of tree (much faster if density field reasonably uniform == true if no gravity)
- rearrangement of SPH equations so only one loop over the particles is required, plus efficient use of neighbour cache to speed up calculations
- factor of ~10 faster than “standard” SPH codes (Kitsionas et al. 2009)
- implements full “variable smoothing length” SPH c.f. Springel & Hernquist (2002), Monaghan (2002), Price & Monaghan (2004,2007)

Initial conditions

$$l_x = \begin{cases} 0 & \text{for } R < R_1 \\ \frac{A}{2}\left[1 + \sin\left(\pi \frac{R - R_0}{R_2 - R_1}\right)\right] & \text{for } R_1 < R < R_2 \\ A & \text{for } R > R_2 \end{cases}$$

A=0.01

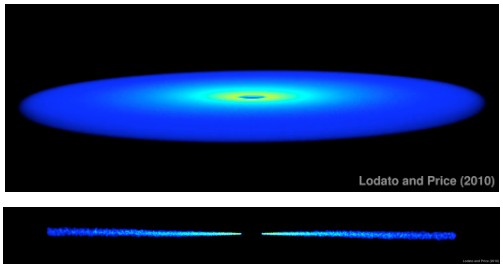

A=0.5

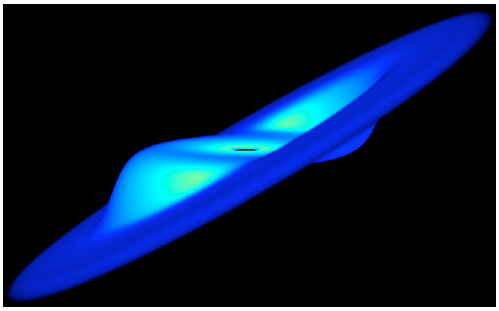

Require high resolution to resolve disc scale height

Simulations: low amplitude

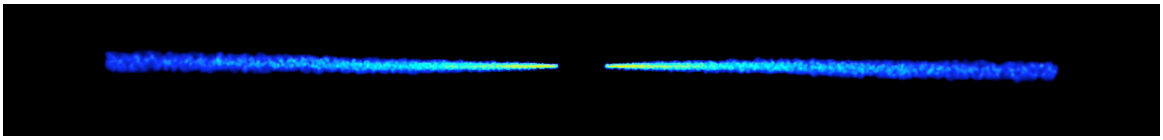

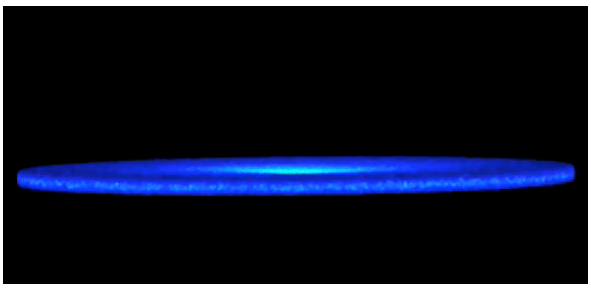

Simulations (high amplitude)

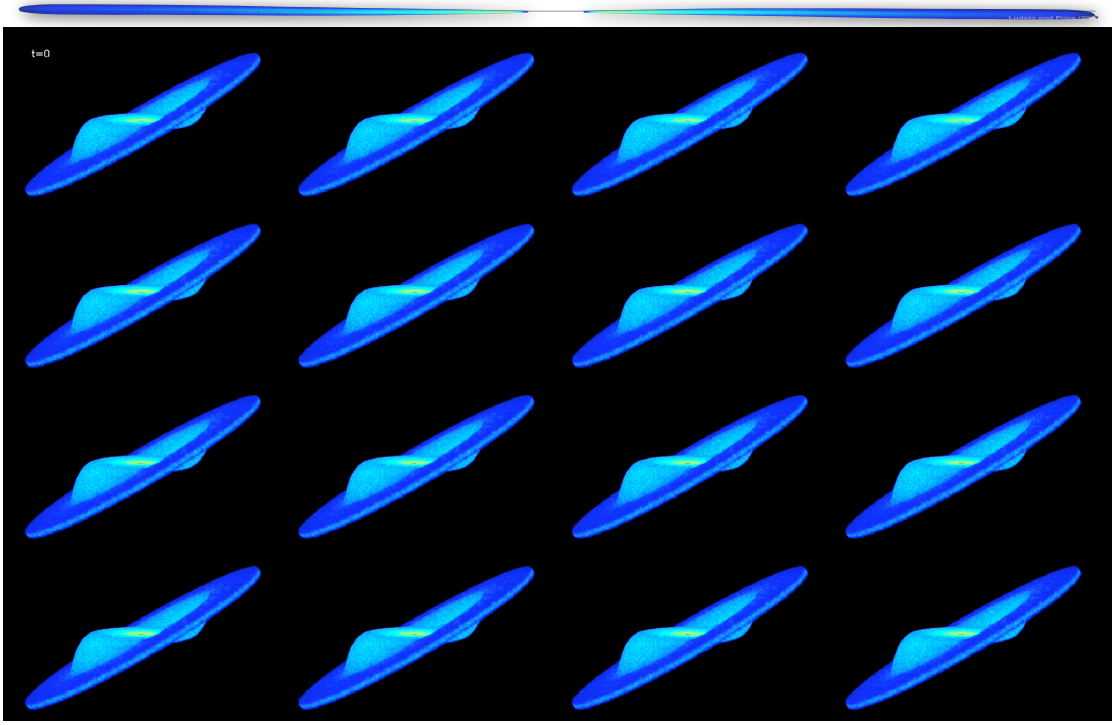

Comparison with theory

- Compare to a one-dimensional disc evolution with fixed diffusion parameters for the disc and the warp, i.e.:

$$\begin{aligned}\frac{\partial \mathbf{L}}{\partial t} = & \quad \frac{3}{R}\frac{\partial}{\partial R}\left[\frac{R^{1/2}}{\Sigma}\frac{\partial}{\partial R}(\nu_1 \Sigma R^{1/2})\mathbf{L}\right] \\ & + \frac{1}{R}\frac{\partial}{\partial R}\left[\left(\nu_2 R^2 \left|\frac{\partial \mathbf{l}}{\partial R}\right|^2 - \frac{3}{2}\nu_1\right)\mathbf{L}\right] \\ & + \frac{1}{R}\frac{\partial}{\partial R}\left(\frac{1}{2}\nu_2 R|\mathbf{L}|\frac{\partial \mathbf{l}}{\partial R}\right).\end{aligned}$$

Measuring the diffusion of a warp

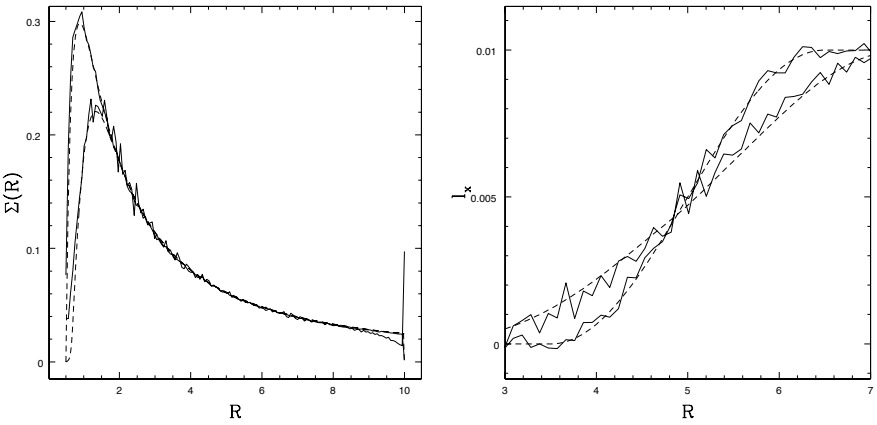

Figure 3. Evolution of simulation S11. The solid lines refer to the azimuthal and vertical average of the SPH simulation, while the dashed lines show the evolution of the corresponding initial conditions obtained by applying equations (8) and (9) for the warp, while the surface density is evolved using a viscosity parameter $\alpha = 0.08$. The left-hand panel shows the evolution of the surface density Σ, while the right-hand panel shows the evolution of l_x. The different lines refer to $t = 0$ and 155 (in units of the dynamical time at $R = 1$).

Comparison with 1/(2α) theory (Lodato & Pringle 2007)

Implies excess dissipation in the disc (higher alpha than nominally input value)

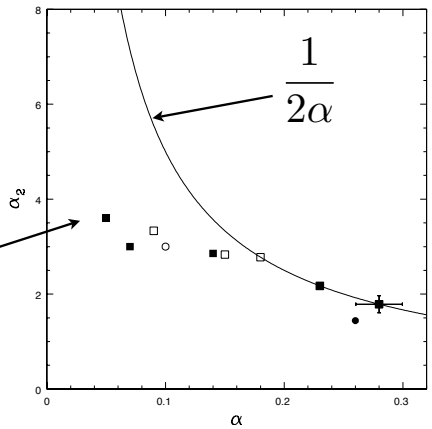

Figure 8. Results of the numerical simulations. The points indicate the values of the diffusion coefficient α_2 as a function of the viscosity coefficient α. The solid symbols refer to simulations that do not use the 'viscous switch' and should thus have a viscosity more closely approximating Navier–Stokes. The open symbols do use the viscous switch. The squares refer to the small warp amplitude case $\psi_{\max} \approx 0.026$, while the circles refer to the large amplitude case $\psi_{\max} \approx 1.3$. The error bars shown represent the typical uncertainties on the diffusion coefficients. The solid line shows the expected value of α_2 from the linear theory. It is evident that our simulations reproduce the expected results from linear theory for values of $\alpha > 0.16$. Below this value we find that α_2 appears to saturate at a value around $\alpha_{\max} \sim 3$–4.

What's going wrong?

- Development of supersonic motions at low alpha giving excess dissipation compared to theory?
- Numerical resolution?
- Something funny with the fitting procedure used to measure alpha and alpha2?
- Effect of the viscosity formulation used in the SPH code?
- Is the right theory being applied?

Calibration of alpha

- replace "by-eye" fitting with repeatable, quantitative procedure

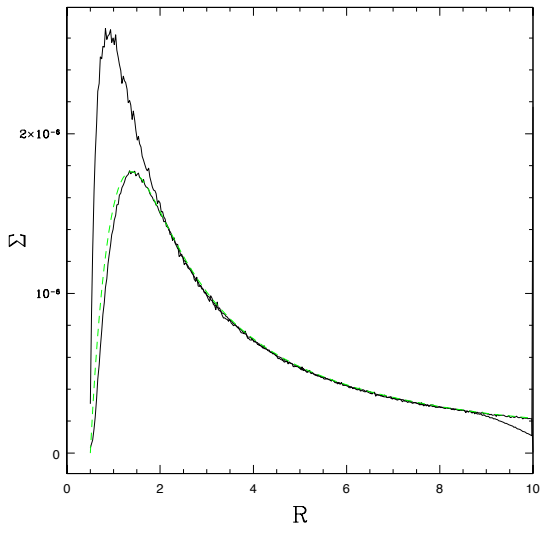

$$E_\alpha = \sum_i [\Sigma_i - \Sigma^{1\mathrm{D}}(R_i)]^2,$$

$$\begin{aligned} \alpha_{n+1} &= \alpha_n - \frac{E'_\alpha(\alpha_n)}{E''_\alpha(\alpha_n)} \\ &= \alpha_n - \frac{\epsilon}{2}\left[\frac{E_\alpha(\alpha_n+\epsilon) - E_\alpha(\alpha_n-\epsilon)}{E_\alpha(\alpha_n+\epsilon) + E_\alpha(\alpha_n-\epsilon) - 2E_\alpha(\alpha_n)}\right]. \end{aligned}$$

Calibration of the disc viscosity

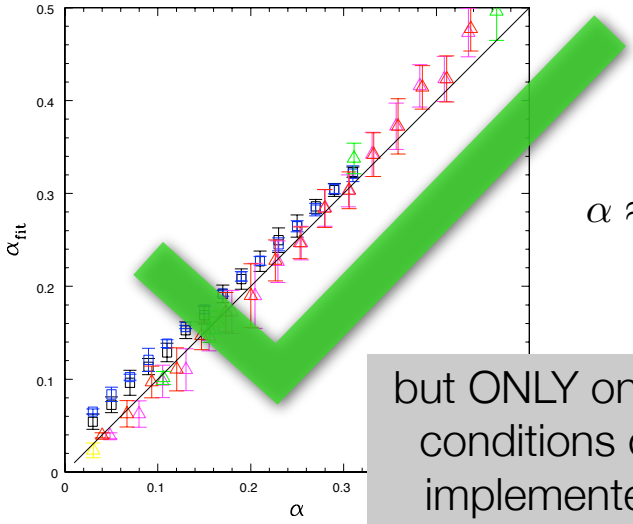

$$\alpha \approx \frac{1}{10}\alpha^{\rm AV}\frac{\langle h\rangle}{H},$$

but ONLY once boundary conditions on 1D code implemented correctly

Figure 4. Comparison between the input value of α and the measured value obtained fitting the SPH data to the 1D evolution of Σ, with the zero torque boundary condition enforced exactly. Results are shown with triangles for

Measurement of α_2 as a function of α

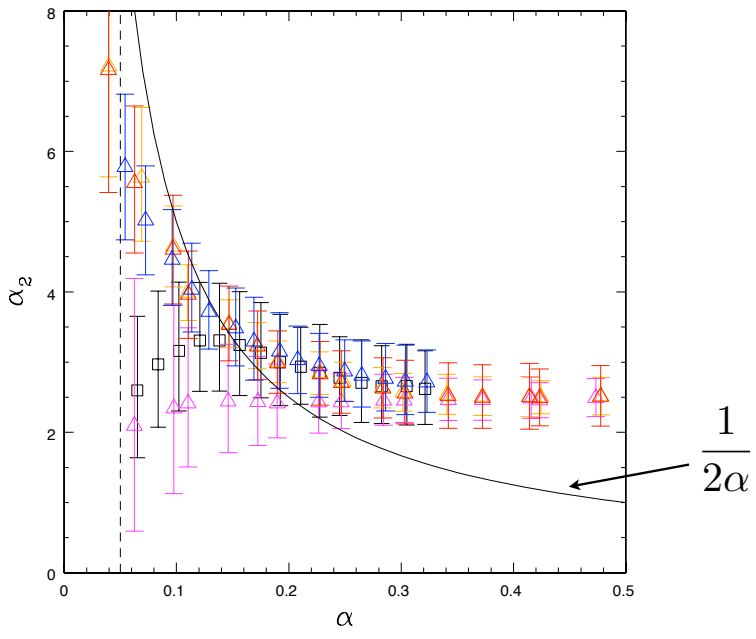

Results

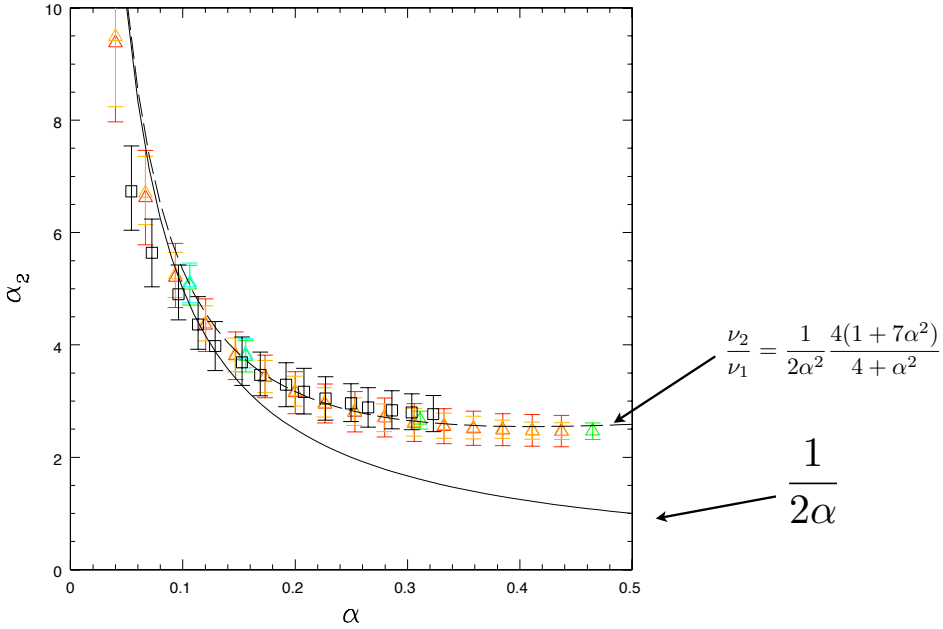

Ogilvie (1999)'s non-linear theory

Equation (38) at $O(\epsilon^{s+3})$:

$$\Big(\Omega\partial_\phi - \frac{v_{\theta1}}{r}\partial_{\bar\zeta}\Big)p_1 + \Big(v_{r1}\partial_r - \frac{v_{\theta2}}{r}\partial_{\bar\zeta} + \frac{v_{\phi1}}{r}\partial_\phi\Big)p_0 = \frac{\Gamma p_1}{r}\partial_{\bar\zeta}v_{\theta1} - \Gamma p_0\Big[\frac{1}{r^2}\partial_r(r^2v_{r1}) - \frac{1}{r}\partial_{\bar\zeta}v_{\theta2} + \frac{1}{r}\partial_\phi v_{\phi1}\Big]. \tag{74}$$

Equation (41) at $O(\epsilon^{s+2})$:

$$\begin{aligned}
&\rho_0\Big(\Omega\partial_\phi - \frac{v_{\theta1}}{r}\partial_{\bar\zeta}\Big)v_{r2} + \rho_0\Big(v_{r1}\partial_r - \frac{v_{\theta2}}{r}\partial_{\bar\zeta} + \frac{v_{\phi1}}{r}\partial_\phi\Big)v_{r1} + \rho_1\Big(\Omega\partial_\phi - \frac{v_{\theta1}}{r}\partial_{\bar\zeta}\Big)v_{r1} - \frac{\rho_0}{r}\big[v_{\theta1} + rv_{r1}(\beta'\cos\phi + \gamma'\sin\beta\sin\phi)\big]^2\\
&- 2\rho_0\Omega\Big[-\frac{1}{2}r\Omega\bar\zeta^2 + v_{\phi2} + r(\dot\gamma + v_{r2}\gamma')\cos\beta - rv_{r1}(\beta'\sin\phi - \gamma'\sin\beta\cos\phi)\bar\zeta\Big] - \frac{\rho_0}{r}(v_{\phi1} + rv_{r1}\gamma'\cos\beta)^2\\
&- 2\rho_1\Omega(v_{\phi1} + rv_{r1}\gamma'\cos\beta) = -(\beta'\cos\phi + \gamma'\sin\beta\sin\phi)\partial_{\bar\zeta}\Big\{p_1 - \Big(\mu_{b0} + \frac{1}{3}\mu_0\Big)\Big[\frac{1}{r^2}\partial_r(r^2v_{r1}) - \frac{1}{r}\partial_{\bar\zeta}v_{\theta2} + \frac{1}{r}\partial_\phi v_{\phi1}\Big]\\
&+ \Big(\mu_{b1} + \frac{1}{3}\mu_1\Big)\frac{1}{r}\partial_{\bar\zeta}v_{\theta1}\Big\} - (\partial_r - \gamma'\cos\beta\,\partial_\phi)\Big[p_0 + (\mu_{b0} + \frac{1}{3}\mu_0)\frac{1}{r}\partial_{\bar\zeta}v_{\theta1}\Big]\\
&+ \Big[\frac{1}{r^2} + (\beta'\cos\phi + \gamma'\sin\beta\sin\phi)^2\Big]\partial_{\bar\zeta}(\mu_0\partial_{\bar\zeta}v_{r2} + \mu_1\partial_{\bar\zeta}v_{r1}) + (\beta'\cos\phi + \gamma'\sin\beta\sin\phi)\partial_{\bar\zeta}\big[\mu_0(\partial_r - \gamma'\cos\beta\,\partial_\phi)v_{r1}\big]\\
&+ \frac{1}{r^2}(\partial_r - \gamma'\cos\beta\,\partial_\phi)\big[\mu_0r^2(\beta'\cos\phi + \gamma'\sin\beta\sin\phi)\partial_{\bar\zeta}v_{r1}\big] - \frac{2v_{r1}}{r}(\beta'\cos\phi + \gamma'\sin\beta\sin\phi)\partial_{\bar\zeta}\mu_0\\
&+ \frac{1}{r^3}\big[(\partial_r - \gamma'\cos\beta\,\partial_\phi)(\mu_0r^2)\big]\partial_{\bar\zeta}\big[v_{\theta1} + rv_{r1}(\beta'\cos\phi + \gamma'\sin\beta\sin\phi)\big]\\
&- (\partial_{\bar\zeta}\mu_0)(\partial_r - \gamma'\cos\beta\,\partial_\phi)\Big[\frac{v_{\theta1}}{r} + v_{r1}(\beta'\cos\phi + \gamma'\sin\beta\sin\phi)\Big]\\
&- \frac{1}{r}(\partial_{\bar\zeta}\mu_0)\partial_\phi\big[(\beta'\cos\phi + \gamma'\sin\beta\sin\phi)(v_{\phi1} + rv_{r1}\gamma'\cos\beta)\big] + \Omega'\partial_\phi\mu_0\\
&+ \frac{1}{r}(\beta'\cos\phi + \gamma'\sin\beta\sin\phi)(\partial_\phi\mu_0)\partial_{\bar\zeta}(v_{\phi1} + rv_{r1}\gamma'\cos\beta) + \Omega(\beta'\sin\phi - \gamma'\sin\beta\cos\phi)\partial_{\bar\zeta}\mu_1.
\end{aligned} \tag{75}$$

Equation (42) at $O(\epsilon^{s+2})$:

$$\begin{aligned}
&\rho_0\Big(\Omega\partial_\phi - \frac{v_{\theta1}}{r}\partial_{\bar\zeta}\Big)\big[v_{\theta2} + r(\dot\beta + v_{r2}\beta')\cos\phi + r(\dot\gamma + v_{r2}\gamma')\sin\beta\sin\phi\big]\\
&+ \rho_0\Big(v_{r1}\partial_r - \frac{v_{\theta2}}{r}\partial_{\bar\zeta} + \frac{v_{\phi1}}{r}\partial_\phi\Big)\big[v_{\theta1} + rv_{r1}(\beta'\cos\phi + \gamma'\sin\beta\sin\phi)\big]
\end{aligned}$$

$$
\begin{aligned}
&+\frac{1}{r^2}(\partial_r-\gamma'\cos\beta\,\partial_\phi)\big[\mu_0 r^2(\beta'\cos\phi+\gamma'\sin\beta\sin\phi)\partial_{\tilde\zeta}v_{r1}\big]-\frac{2v_{r1}}{r}(\beta'\cos\phi+\gamma'\sin\beta\sin\phi)\partial_{\tilde\zeta}\mu_0\\
&+\frac{1}{r^3}\big[(\partial_r-\gamma'\cos\beta\,\partial_\phi)(\mu_0 r^2)\big]\partial_{\tilde\zeta}\big[v_{\theta1}+rv_{r1}(\beta'\cos\phi+\gamma'\sin\beta\sin\phi)\big]\\
&-(\partial_{\tilde\zeta}\mu_0)(\partial_r-\gamma'\cos\beta\,\partial_\phi)\Big[\frac{v_{\theta1}}{r}+v_{r1}(\beta'\cos\phi+\gamma'\sin\beta\sin\phi)\Big]\\
&-\frac{1}{r}(\partial_{\tilde\zeta}\mu_0)\partial_\phi\big[(\beta'\cos\phi+\gamma'\sin\beta\sin\phi)(v_{\phi1}+rv_{r1}\gamma'\cos\beta)\big]+\Omega'\partial_\phi\mu_0\\
&+\frac{1}{r}(\beta'\cos\phi+\gamma'\sin\beta\sin\phi)(\partial_\phi\mu_0)\partial_{\tilde\zeta}(v_{\phi1}+rv_{r1}\gamma'\cos\beta)+\Omega(\beta'\sin\phi-\gamma'\sin\beta\cos\phi)\partial_{\tilde\zeta}\mu_1. \qquad (75)
\end{aligned}
$$

Equation (42) at $O(\epsilon^{s+2})$:

$$
\begin{aligned}
&\rho_0\Big(\Omega\partial_\phi-\frac{v_{\theta1}}{r}\partial_{\tilde\zeta}\Big)\big[v_{\theta2}+r(\dot\beta+v_{r2}\beta')\cos\phi+r(\dot\gamma+v_{r2}\gamma')\sin\beta\sin\phi\big]\\
&+\rho_0\Big(v_{r1}\partial_r-\frac{v_{\theta2}}{r}\partial_{\tilde\zeta}+\frac{v_{\phi1}}{r}\partial_\phi\Big)\big[v_{\theta1}+rv_{r1}(\beta'\cos\phi+\gamma'\sin\beta\sin\phi)\big]\\
&+\rho_1\Big(\Omega\partial_\phi-\frac{v_{\theta1}}{r}\partial_{\tilde\zeta}\Big)\big[v_{\theta1}+rv_{r1}(\beta'\cos\phi+\gamma'\sin\beta\sin\phi)\big]+\frac{\rho_0 v_{r1}}{r}\big[v_{\theta1}+rv_{r1}(\beta'\cos\phi+\gamma'\sin\beta\sin\phi)\big]\\
&-\rho_0\Omega\big[(v_{\phi1}+rv_{r1}\gamma'\cos\beta)\zeta+r(\dot\beta+v_{r2}\beta')\sin\phi-r(\dot\gamma+v_{r2}\gamma')\sin\beta\cos\phi\big]\\
&-\frac{\rho_0}{r}(v_{\phi1}+rv_{r1}\gamma'\cos\beta)\big[r\Omega\zeta+rv_{r1}(\beta'\sin\phi-\gamma'\sin\beta\cos\phi)\big]-\rho_1\Omega\big[r\Omega\zeta+rv_{r1}(\beta'\sin\phi-\gamma'\sin\beta\cos\phi)\big]\\
&=\frac{1}{r}\partial_{\tilde\zeta}\Big\{p_1-\Big(\mu_{b0}+\frac{1}{3}\mu_0\Big)\Big[\frac{1}{r^2}\partial_r(r^2v_{r1})-\frac{1}{r}\partial_{\tilde\zeta}v_{\theta2}+\frac{1}{r}\partial_\phi v_{\phi1}\Big]+\Big(\mu_{b1}+\frac{1}{3}\mu_1\Big)\frac{1}{r}\partial_{\tilde\zeta}v_{\theta1}\Big\}\\
&+\Big[\frac{1}{r^2}+(\beta'\cos\phi+\gamma'\sin\beta\sin\phi)^2\Big]\partial_{\tilde\zeta}\big\{\mu_0\partial_{\tilde\zeta}\big[v_{\theta2}+r(\dot\beta+v_{r2}\beta')\cos\phi+r(\dot\gamma+v_{r2}\gamma')\sin\beta\sin\phi\big]\\
&+\mu_1\partial_{\tilde\zeta}\big[v_{\theta1}+rv_{r1}(\beta'\cos\phi+\gamma'\sin\beta\sin\phi)\big]\big\}\\
&+(\beta'\cos\phi+\gamma'\sin\beta\sin\phi)\partial_{\tilde\zeta}\big\{\mu_0(\partial_r-\gamma'\cos\beta\,\partial_\phi)\big[v_{\theta1}+rv_{r1}(\beta'\cos\phi+\gamma'\sin\beta\sin\phi)\big]\big\}\\
&+\frac{1}{r^2}(\partial_r-\gamma'\cos\beta\,\partial_\phi)\big\{\mu_0 r^2(\beta'\cos\phi+\gamma'\sin\beta\sin\phi)\partial_{\tilde\zeta}\big[v_{\theta1}+rv_{r1}(\beta'\cos\phi+\gamma'\sin\beta\sin\phi)\big]\big\}\\
&-\frac{1}{r}(\beta'\cos\phi+\gamma'\sin\beta\sin\phi)(\partial_{\tilde\zeta}\mu_0)\big[v_{\theta1}+rv_{r1}(\beta'\cos\phi+\gamma'\sin\beta\sin\phi)\big]-\frac{1}{r^3}(\partial_{\tilde\zeta}v_{r1})(\partial_r-\gamma'\cos\beta\,\partial_\phi)(\mu_0r^2)\\
&+\frac{1}{r}(\partial_{\tilde\zeta}\mu_0)(\partial_r-\gamma'\cos\beta\,\partial_\phi)v_{r1}+\frac{1}{r^3}(\partial_{\tilde\zeta}\mu_0)\partial_\phi(v_{\phi1}+rv_{r1}\gamma'\cos\beta)\\
&-\frac{1}{r^2}(\partial_\phi\mu_0)\partial_{\tilde\zeta}(v_{\phi1}+rv_{r1}\gamma'\cos\beta)-(\beta'\sin\phi-\gamma'\sin\beta\cos\phi)(\beta'\cos\phi+\gamma'\sin\beta\sin\phi)\partial_{\tilde\zeta}\big[\mu_0(v_{\phi1}+rv_{r1}\gamma'\cos\beta)\big]\\
&-r\Omega(\beta'\sin\phi-\gamma'\sin\beta\cos\phi)(\beta'\cos\phi+\gamma'\sin\beta\sin\phi)\partial_{\tilde\zeta}\mu_1-\frac{1}{r^2}(\partial_r-\gamma'\cos\beta\,\partial_\phi)\big[\mu_0r^3\Omega(\beta'\sin\phi-\gamma'\sin\beta\cos\phi)\big]\\
&-\mu_0(\beta'\sin\phi-\gamma'\sin\beta\cos\phi)\big[(r\Omega)'+(\beta'\cos\phi+\gamma'\sin\beta\sin\phi)\partial_{\tilde\zeta}(v_{\phi1}+rv_{r1}\gamma'\cos\beta)\big]. \qquad (76)
\end{aligned}
$$

Equation (43) at $O(\epsilon^{s+2})$:

$$
\begin{aligned}
&\rho_0\Big(\Omega\partial_\phi-\frac{v_{\theta1}}{r}\partial_{\tilde\zeta}\Big)\Big[v_{\phi2}-\frac{1}{2}r\Omega\zeta^2+r(\dot\gamma+v_{r2}\gamma'\cos\beta)-rv_{r1}(\beta'\sin\phi-\gamma'\sin\beta\cos\phi)\zeta\Big]\\
&+\rho_0\Big(v_{r1}\partial_r-\frac{v_{\theta2}}{r}\partial_{\tilde\zeta}+\frac{v_{\phi1}}{r}\partial_\phi\Big)(v_{\phi1}+rv_{r1}\gamma'\cos\beta)+\rho_1\Big(\Omega\partial_\phi-\frac{v_{\theta1}}{r}\partial_{\tilde\zeta}\Big)(v_{\phi1}+rv_{r1}\gamma'\cos\beta)+\frac{\rho_0\kappa^2}{2\Omega}v_{r2}+\frac{\rho_1\kappa^2}{2\Omega}v_{r1}\\
&+\frac{\rho_0}{r}v_{r1}(v_{\phi1}+rv_{r1}\gamma'\cos\beta)+\frac{\rho_0}{r}\big[v_{\theta1}+rv_{r1}(\beta'\cos\phi+\gamma'\sin\beta\sin\phi)\big]\big[r\Omega\zeta+rv_{r1}(\beta'\sin\phi-\gamma'\sin\beta\cos\phi)\big]\\
&=-\frac{1}{r}\partial_\phi\Big[p_0+\Big(\mu_{b0}+\frac{1}{3}\mu_0\Big)\frac{1}{r}\partial_{\tilde\zeta}v_{\theta1}\Big]+r\Omega'(\beta'\cos\phi+\gamma'\sin\beta\sin\phi)\partial_{\tilde\zeta}\mu_1\\
&+\frac{1}{r^2}\partial_r\big[\mu_0r^2(r\Omega)'\big]-r\Omega(\partial_\phi\mu_0)\gamma'\cos\beta+(\beta'\cos\phi+\gamma'\sin\beta\sin\phi)\partial_{\tilde\zeta}\big[\mu_0(\partial_r-\gamma'\cos\beta\,\partial_\phi)(v_{\phi1}+rv_{r1}\gamma'\cos\beta)\big]\\
&+\frac{1}{r^2}(\partial_r-\gamma'\cos\beta\,\partial_\phi)\big[\mu_0r^2(\beta'\cos\phi+\gamma'\sin\beta\sin\phi)\partial_{\tilde\zeta}(v_{\phi1}+rv_{r1}\gamma'\cos\beta)\big]\\
&+\Big[\frac{1}{r^2}+(\beta'\cos\phi+\gamma'\sin\beta\sin\phi)^2\Big]\partial_{\tilde\zeta}\Big\{\mu_0\partial_{\tilde\zeta}\Big[-\frac{1}{2}r\Omega\zeta^2+v_{\phi2}+r(\dot\gamma+v_{r2}\gamma')\cos\beta-rv_{r1}(\beta'\sin\phi-\gamma'\sin\beta\cos\phi)\zeta\Big]\\
&+\mu_1\partial_{\tilde\zeta}(v_{\phi1}+rv_{r1}\gamma'\cos\beta)\big\}-\frac{\Omega}{r}\partial_r(\mu_0r)-\frac{1}{r}(v_{\phi1}+rv_{r1}\gamma'\cos\beta)(\beta'\cos\phi+\gamma'\sin\beta\sin\phi)\partial_{\tilde\zeta}\mu_0\\
&+\frac{\Omega}{r}\zeta\partial_{\tilde\zeta}\mu_0+\frac{1}{r}(\partial_\phi v_{r1})(\beta'\cos\phi+\gamma'\sin\beta\sin\phi)\partial_{\tilde\zeta}\mu_0-\frac{1}{r}(\partial_\phi\mu_0)(\beta'\cos\phi+\gamma'\sin\beta\sin\phi)\partial_{\tilde\zeta}v_{r1}\\
&-\frac{1}{r^2}(\partial_{\tilde\zeta}\mu_0)\partial_\phi\big[v_{\theta1}+rv_{r1}(\beta'\cos\phi+\gamma'\sin\beta\sin\phi)\big]+\frac{1}{r^2}(\partial_\phi\mu_0)\partial_{\tilde\zeta}\big[v_{\theta1}+rv_{r1}(\beta'\cos\phi+\gamma'\sin\beta\sin\phi)\big]\\
&+(\beta'\sin\phi-\gamma'\sin\beta\cos\phi)(\beta'\cos\phi+\gamma'\sin\beta\sin\phi)\partial_{\tilde\zeta}\big\{\mu_0\big[v_{\theta1}+rv_{r1}(\beta'\cos\phi+\gamma'\sin\beta\sin\phi)\big]\big\}\\
&+\mu_0(\beta'\sin\phi-\gamma'\sin\beta\cos\phi)(\beta'\cos\phi+\gamma'\sin\beta\sin\phi)\partial_{\tilde\zeta}\big[v_{\theta1}+rv_{r1}(\beta'\cos\phi+\gamma'\sin\beta\sin\phi)\big]\\
&-\mu_0r\Omega(\beta'\sin\phi-\gamma'\sin\beta\cos\phi)^2. \qquad (77)
\end{aligned}
$$

4.4 Integrated quantities

Finally, equation (37) is also required at $O(\epsilon^{s+2})$, but only in its integrated form,[2]

$$\partial_t\Big(\int\!\!\int\rho_0\,r\,\mathrm{d}\phi\,\mathrm{d}\tilde\zeta\Big)+\frac{1}{r}\partial_r\Big[r\int\!\!\int(\rho_0v_{r2}+\rho_1v_{r1})\,r\,\mathrm{d}\phi\,\mathrm{d}\tilde\zeta\Big]=0. \qquad (78)$$

The surface density $\Sigma(r,T)$ at leading order in ϵ is

$$\Sigma=\int\rho_0\,r\,\mathrm{d}\tilde\zeta, \qquad (79)$$

and is independent of ϕ by virtue of equation (68). Other vertically integrated quantities are non-axisymmetric, however, and these will be written with tildes. The corresponding azimuthally averaged quantities, written without tildes, are defined by the operation

$$\langle\cdot\rangle=\frac{1}{2\pi}\int\cdot\,\mathrm{d}\phi. \qquad (80)$$

Thus a suitably averaged radial velocity $\bar v_r(r,T)$ may be defined by

$$\Sigma\bar v_r=\mathscr{F}=\langle\tilde{\mathscr{F}}\rangle, \qquad (81)$$

where

$$\tilde{\mathscr{F}}=\int(\rho_0v_{r2}+\rho_1v_{r1})\,r\,\mathrm{d}\tilde\zeta \qquad (82)$$

is the radial mass flux at $O(\epsilon^{s+3})$.[3] Then equation (78), divided by 2π, reads

$$\partial_t\Sigma+\frac{1}{r}\partial_r(r\Sigma\bar v_r)=0, \qquad (83)$$

which agrees with equation (2). Two more definitions will be useful. A suitably averaged kinematic viscosity $\bar\nu(r,T)$ may be defined by

$$\bar\nu\Sigma=\mathscr{V}=\langle\tilde{\mathscr{V}}\rangle \qquad (84)$$

[2]Throughout this paper, integrations with respect to ϕ are carried out from 0 to 2π, and integrations with respect to $\tilde\zeta$ are carried out over the full vertical extent of the disc.

Large amplitude warps (high disc viscosity)

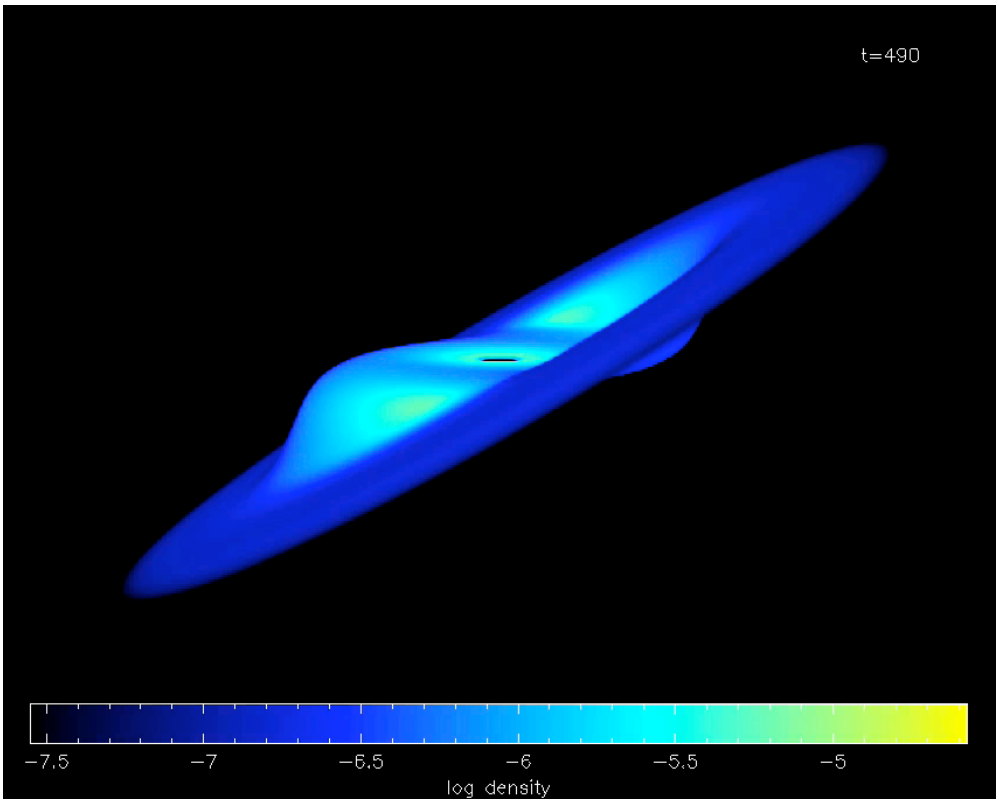

Effect of warp amplitude

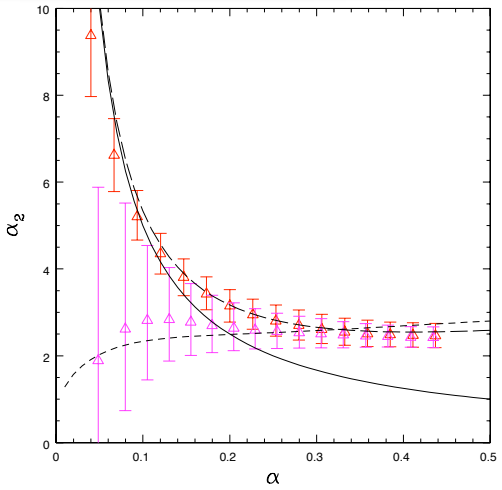

Figure 8. Relation between the warp diffusion coefficient α_2 and α for large amplitude warps. The magenta triangles show the results for $A = 0.5$, while the red triangles, for comparison, indicate the small amplitude ($A = 0.01$) case. The solid and long-dashed lines show the $1/(2\alpha)$ relation and the corrections expected for finite α, respectively. The short-dashed line shows the expected relation based on the non-linear theory of O99, assuming a fixed $\psi = 0.55$ (roughly comparable to the average ψ value

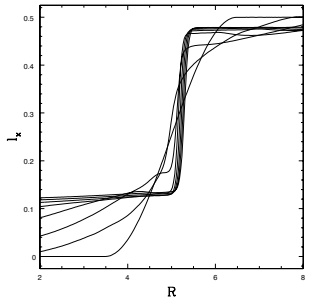

Figure 10. Shell averaged profiles of l_x from the SPH simulation (black lines) at intervals of $\Delta t = 500$ up to $t = 3500$ (in code units), for the low viscosity case $\alpha = 0.03$, using 20 million particles and a strongly non-linear warp amplitude ($A = 0.5$). The large warp amplitude simulations at low α show a strong steepening effect in the warp profile because different parts of the warp propagate at different speeds. We have been unable to run the appropriate nonlinear solution for this case because the steepening causes unphysical oscillations in the one dimensional code.

Large amplitude warps (low disc viscosity)

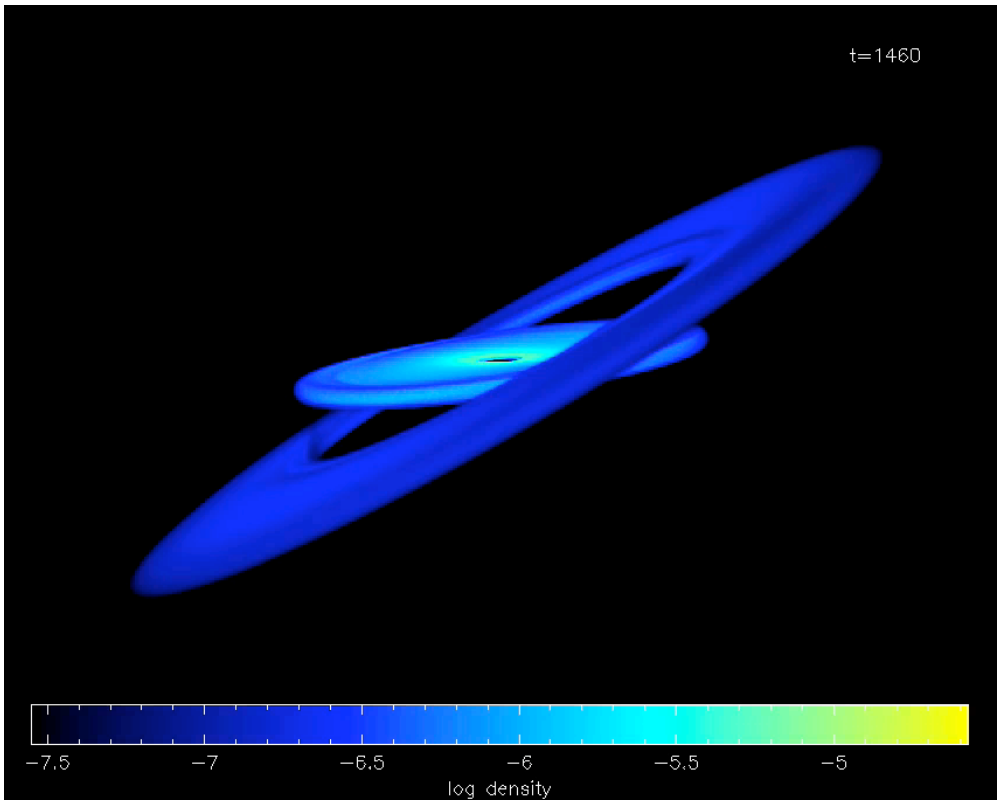

Higher order terms: Precession

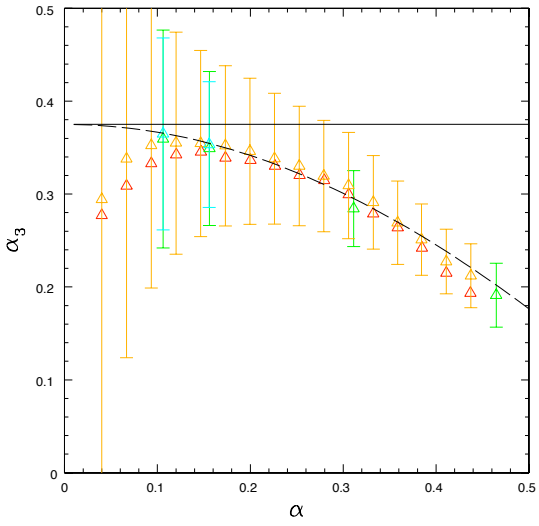

Figure 13. Relation between the precession coefficient α_3 and the disc viscosity α, for warp amplitudes $A = 0.01$ (red and green triangles) and $A = 0.05$ (orange and cyan triangles). All calculations employ 2 million

Precession with non-linear warps

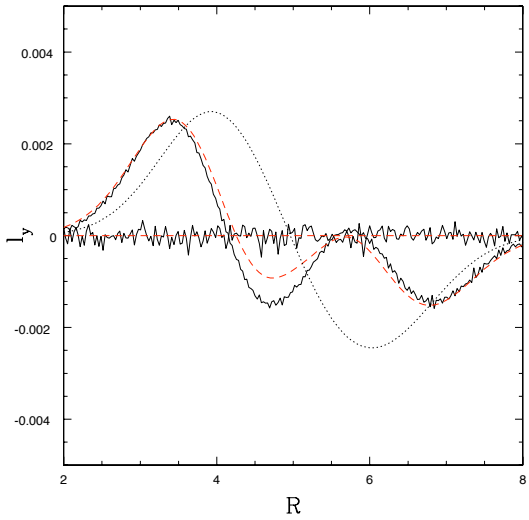

Figure 14. Profile of l_y at $t = 500$ time units for the case $A = 0.5$ and $\alpha = 0.43$. The solid black lines refer to the SPH simulations, while the dashed red line show the result of the evolution of the diffusion plus precession code, with non linear warp parameter α_2 and α_3 computed based on O99 theory of warp propagation. For comparison, we also show with the dotted black line the profile at $t = 500$ obtained from the simple 1D evolution

So what?

- We find spectacular agreement between the 3D SPH simulations and both the linear and non-linear theory of warp propagation
- alpha2 = 1/(2 alpha) only true for very low viscosity discs and very low amplitude warps
- much slower propagation found for large amplitude warps, in agreement with theory
- excitation of large amplitude warps in low viscosity discs will steepen and can result in almost-complete disc break
- SPH is a great method to use for simulating accretion discs